Ballistic deposition on surfaces

Paul Meakin
Central Research and Development Department, E.I. duPont de Nemours and Company, Experimental Station, Wilmington, Delaware 19898

P. Ramanlal and L. M. Sander
Department of Physics, University of Michigan, Ann Arbor, Michigan 48109

R. C. Ball
Cavendish Laboratory, Madingly Road, Cambridge CB3 0HE, England
(Received 2 June 1986)

We consider several aspects of the irreversible deposition of particles on surfaces. We show by direct numerical simulation that the well-known "tangent rule" for the orientation of the columnar microstructure is only qualitatively correct. We demonstrate that the interface width of the deposit for normal incidence scales according to the hypothesis of Family and Vicsek. This means that the width scales as $\bar{h}^{\nu}$ for short times and l^{α} for the steady state where $\bar{h}$ is the mean height and l the width. We find by simulation $\nu \simeq \frac{1}{3}, \alpha \simeq \frac{1}{2}$ in two dimensions (2D) and $\nu \simeq \frac{1}{4}, \alpha \simeq \frac{1}{3}$ in 3D. We give an analytic treatment which maps the problem onto a spin model. We find $\nu = \frac{1}{3}, \alpha = \frac{1}{2}$ for 2D in agreement with our simulations but $\nu = 0, \alpha = 0$ for 3D.

I. INTRODUCTION

In recent years considerable interest has developed in the formation of random structures under nonequilibrium conditions. Much of our understanding of the geometry of these structures and its relationship to their formation mechanism has come from the study of simple models by means of both computer simulation and theoretical methods. One of the most fundamental of these models is the ballistic-aggregation model in which particles are added to a growing structure via linear (ballistic) trajectories. Other simple models which have been studied intensively include the Eden[1] model, diffusion-limited aggregation[2] (DLA), and diffusion-limited cluster-cluster aggregation.[3,4] Each of these models was originally developed to explore cluster growth and later modified to study growth from surfaces.

The ballistic aggregation model was first developed by Vold[5] and Sutherland[6] in order to develop a better understanding of colloidal aggregation. In this model particles are added one at a time to a growing cluster or aggregate of particles using linear trajectories which have randomly selected positions and directions. In the most extensively studied version of this model the particles are hyperspherical and all of the same size. This model leads to clusters with a complex porous structure which has sometimes been described in terms of a fractal dimensionality[7] (D) which is smaller than the Euclidean dimensionality (d) of the space in which the simulation is carried out. However, based on recent larger-scale computer simulations[8,9] and theoretical arguments[10] a consensus that the fractal dimensionality of ballistic aggregates is equal to their Euclidean dimensionality has now developed. This means that the internal structure of ballistic aggregates is uniform on all but short-length scales. Ballistic addition of particles to a growing cluster does not provide a realistic model for colloidal aggregation. However, this model did provide an important step towards the development of more successful models for colloidal aggregation.[3,4,11,12]

Although Vold[13] did study the deposition of particles onto surfaces, most of the early work on ballistic aggregation was concerned with cluster formation. More recently the development of processes for the manufacture of optical and electronic devices using vapor deposition has stimulated interest in ballistic deposition onto surfaces. One of the main objectives of this work has been to develop a better understanding and control over the characteristic columnar morphology[14–19] which is associated with vapor-deposition processes. This columnar morphology is observed in both two-dimensional (2D) and 3D computer simulations[20] and experiments and is most distinctive when the particles are all added via ballistic trajectories from the same direction with a large angle of incidence (α). In both the experiments and computer simulations it is found that the angle (β) between the growth direction of the columns and the normal to the surface is smaller than the angle of incidence. From careful measurements made on vapor-deposited aluminum films Nieuwenheuzen and Hannstra[18] found that the angle of growth (β) is empirically related to the angle of incidence (α) by

$$\tan(\beta) = \tfrac{1}{2}\tan(\alpha) . \tag{1}$$

This relationship, known as the "tangent rule," was investigated further by Leamy and Dirks[15] using vapor-deposited and sputter-deposited rare-earth-metal —transition-metal thin films. The result obtained by Leamy and Dirks was found, by them, to be consistent with the tangent rule and with 2D and 3D computer simulations.[19,21] While the tangent rule can be supported by

simple arguments based on the idea of shadowing,[22,23] it has not been thoroughly tested using large-scale simulations or established on a rigorous theoretical basis. A mean-field theory of ballistic aggregation has been developed[23] based on the tangent rule. This theory successfully reproduces many of the qualitative features seen in both computer simulations and vapor-deposition experiments.

The universality of the tangent rule has been questioned on the basis of both experimental studies (see, for example, Refs. 24 and 25) and more elaborate and realistic computer models.[15] In this paper we show that the tangent rule is not quantitatively correct even for the most simple off-lattice 2D models for ballistic deposition.

The ballistic-deposition model can be simplified considerably by confining the particles to sites on a square (or cubic) lattice. The particles then follow trajectories which are normal to the surface and stick permanently when they reach an unoccupied site which is "adjacent" (the term adjacent will be precisely defined later) to an occupied site. Since it is necessary to know only the maximum height at which sticking can occur for each of the original surface sites this model can be made very efficient and structures containing more than 10^9 occupied sites can be generated in both two and three dimensions.

Like the off-lattice models these on-lattice ballistic-aggregation (or deposition) models generate porous structures which are uniform on all but short-length scales. However, the active zone[26] (sites at which further growth can occur) exhibits nontrivial scaling behavior. The active zone for two-dimensional square-lattice ballistic deposition was first investigated by Family and Vicsek[27] using deposits grown to a mean height h on strips of width l with periodic boundary conditions in the lateral direction. Family and Vicsek measured the "width of the active zone" (ξ) defined by

$$\xi^2=\frac{1}{l}\sum_{i=1}^{l}(h_i-\bar{h})^2 , \tag{2}$$

where h_i is the height of the active zone at the position of the ith site on the original surface and $\bar{h}$ is the mean height of the active zone. They found that the dependence of ξ on $\bar{h}$ and l could be expressed in terms of the scaling relationship

$$\xi\sim l^{\alpha}f(\bar{h}/l^{\gamma}) , \tag{3}$$

where the scaling function $f(x)$ has the properties $f(x)=$const for large x and $f(x)\sim x^{\nu}$ ($\nu=\alpha/\gamma$) for small x. This means that for small heights ($\bar{h}\ll l$) $\xi\sim\bar{h}^{\nu}$ and for large heights ($\bar{h}\gg l^{\gamma}$) $\xi\sim l^{\alpha}$. From their numerical results Family and Vicsek found that $\alpha=0.42\pm0.03$ and $\nu=0.30\pm0.02$.

It has recently been shown that the width of the active zone[26] for the 2D Eden model with strip geometry can be described by the same scaling form [Eq. (3)] as the ballistic-deposition model with scaling exponents (α and γ) which seem to be approximately equal for both models.[27–31] Recently Kardar, Parisi, and Zhang[32] have proposed a model for the evolution of the active zone for both the Eden growth and ballistic-deposition processes. A Langevin equation is proposed for the local growth of the active zone which leads to the result $\alpha=\frac{1}{2}$ and $\gamma=1.5$ which are consistent with available computer simulation results for both models if the possibility of significant corrections to scaling in the computer simulation results are taken into account. Even for very simple models such as Eden growth and ballistic aggregation, corrections to the asymptotic scaling behavior can be important and have frequently led to erroneous interpretations of computer simulation results.[33] One of the main objectives of the work reported in this paper is to test these ideas using large-scale simulations of ballistic deposition.

If the active zone for ballistic aggregation were a self-similar fractal we would expect to find step sizes in the height of the active zone ($\delta h_i=|h_i-h_{i+1}|$) which could take on arbitrarily large values (for sufficiently large values of $\bar{h}$ and l). Instead we find that the distribution of step sizes (δh) is an exponentially decaying function of δh so that the large step sizes are extremely improbable. In fact, we shall show the step size to be bounded. This means that the active zone of ballistic aggregates should be described in terms of self-affine rather than self-similar fractal geometry.[7,34,35] However, in preference to becoming involved in the niceties and possible controversy of precise terminology we will simply describe what quantities have been measured and what has been found concerning their scaling behavior.

Because of the possible significance of the distribution of step sizes we have also investigated a 2D model in which all the δh values are restricted to a constant value of 1.0. In this model we start with a "surface" which has a height of 0 at odd values of i (the index describing the position along the surface) and 1 at even values of i. Surface sites are then selected randomly and the height is incremented by *two* lattice units if and only if the height of both of the next-nearest neighbors is greater than that of the randomly selected site (i.e., if $h_{i+1}-h_i=1$ and $h_{i-1}-h_i=1$). The extension to 3D is straightforward. The active zone for this model exhibits the scaling behavior given in Eq. (3) with numerical values for the exponents α and γ very close to those predicted by Kardar *et al.*[32] In this paper we show how this modified ballistic-deposition model can be mapped onto a spin exchange model and derive values for the exponents α and γ which are in good agreement with the theoretical results of Kardar *et al.* and with our simulations. In contrast, in 3D our analytic results from the spin exchange model do not agree with simulations or with Ref. 32. (However, Ref. 32 does not agree with our simulations either. The situation in 3D is, at the moment, very puzzling.)

II. SIMULATION METHODS

Efficient computer algorithms for the simulation of off-lattice ballistic aggregation have been described previously.[8] For the purposes of the work described in this paper these algorithms were modified to simulate ballistic deposition in strip geometry with periodic boundary conditions. Particles are started at randomly selected positions at a height of $h_{\max}+1$ particle diameters from the original surface ($h_{\max}$ is the maximum height for the

center of any particle in the deposit which has already grown on the surface). The particles then follow a linear trajectory with a prescribed angle of incidence until they contact either a particle in the deposit or reach the original surface. The particles are stopped at the point where they first make contact and become part of the growing deposit. Most of our 2D simulations using this model were carried out using double-precision arithmetic with a "surface" either 2000 or 4000 particle diameters long (depending on the angle of incidence) and 200 000 particles (disks of unit diameter) were added. Except for very large angles of incidence these simulations required less than $\frac{1}{2}$ h of CPU time on a VAX 8600 computer.

Figure 1 shows an early stage in a 2D simulation of ballistic deposition carried out using the lattice model. Similar models have been described previously[8,9] and only a brief discussion is given here. The sites occupied by the original surface and sites which have already been occupied are indicated as shaded lattice sites. In this particular model, the adjacent unoccupied sites are those which are nearest neighbors to an occupied site and which comprise the active zone (those at the largest height for each position measured along the original surface). They are indicated by a cross ($\times$). This model will be referred to as the nearest-neighbor or NN model. If the next site to be occupied (a site selected at random from those in the active zone) is the one indicated by a circle as well as a cross, then the new active zone sites are those indicated by a circle only. It should be noted that there are always l sites in the active zone and that at most, three active zone sites need to be updated after each growth event. Since we need to record only the height of each of the l sites in the active zone, this algorithm is fast and requires relatively little information storage. Using a relatively inefficient

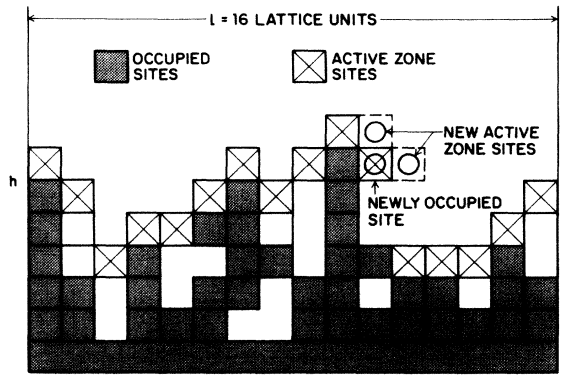

FIG. 1. Schematic representation of a small-scale simulation of ballistic deposition onto a line using a square lattice. Sites occupied by the original surface and the growing deposit are shaded and the sites in the active zones are indicated by crosses. Periodic boundary conditions are used in these simulations and are explicitly shown in the figure. If the site indicated by a cross and a circle is the next to be occupied the two sites indicated by circles alone become new active zone sites and the old active zone sites at the same position (but lower height) disappear from the active zone.

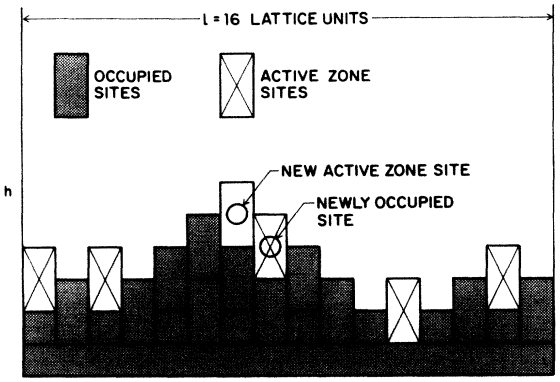

FIG. 2. Schematic representation of a small-scale simulation carried out using the single-step ballistic-deposition model on a square lattice. The sites are labeled in the same way as those in Fig. 1.

random number generator, deposits can be grown (and analyzed) at a rate of about 45 000 sites per second on an IBM 3081 computer.

We have also carried out simulations with a second version of this model in which adjacent sites include both nearest-neighbor and next-nearest-neighbor sites. This model will be referred to as the next-nearest-neighbor or NNN model. Extension of these models to higher dimensions is quite straightforward; we will present results obtained only for the three-dimensional NN model.

Figure 2 shows the "single step" ballistic-deposition model. In this model two sites are added at a randomly selected active site, defined such that the height of the deposit is greater at the two neighboring positions (i.e., $h_{i+i} > h_i$ and $h_{i-i} > h_i$). The simulation starts off with sites of odd index (i) having a height of 0 and those of even index having a height of 1. At this stage there are $l/2$ sites in the active zone. This is the maximum number of sites in the active zone and in general there are considerably fewer (Fig. 2). In this model, the height of the deposit at the ith position always differs from the height of its nearest neighbors by exactly one lattice unit $|h_i - h_{i+1}| = 1$. In 3D we have the same condition with its four next-nearest neighbors. As in our other ballistic-deposition models periodic boundary conditions are used in the lateral directions. In order to improve the efficiency of the program a list of active zone site positions is maintained and updated as the simulation proceeds.

III. RESULTS

A. Tangent rule for 2D off-lattice ballistic deposition

Figure 3 shows the results of a relatively small-scale simulation of 2D off-lattice ballistic deposition using a fixed angle of incidence ($\alpha = 67.5°$) for all of the particles. In this figure the inward pointing arrow indicates the direction of the ballistic trajectories and the outward pointing arrow indicates the angle of growth (β) predicted by the tangent rule [Eq. (1)]. A distinct columnar mor-

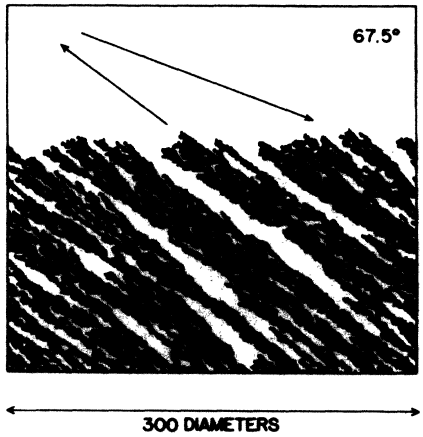

FIG. 3. Results from a small-scale simulation of 2D off-lattice ballistic deposition with an angle of incidence of 67.5. Inward pointing arrow indicates the direction of the incoming particles and the outward pointing arrow indicates the angle of growth predicted by the tangent rule. At this angle of incidence agreement with the tangent rule is quite good but this agreement is not exact and must be regarded as accidental.

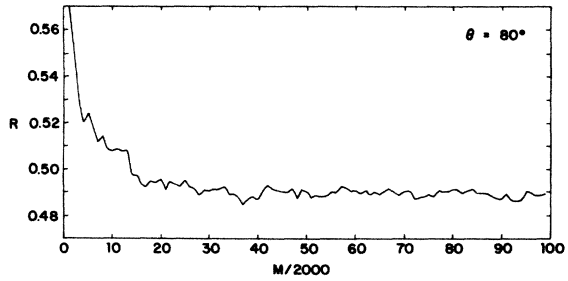

FIG. 4. Dependence of the ratio $R=\langle y_i-y_{i0}\rangle/\langle x_i-x_{i0}\rangle$ on the deposit mass for a 2D off-lattice simulation of deposition onto a line of length 2000 particle diameters using a fixed angle of incidence of 80°.

phology can be seen in this figure and the direction of growth of columns is qualitatively consistent with the tangent rule.

In off-lattice ballistic deposition the incoming particles make contact with only one particle in the deposit (or with the original surface) and the deposit can be considered to consist of "trees" of connected particles with a "root" at the surface. For large angles of incidence these trees may be identified with the columns. In the larger-scale (200 000 particle) simulations the quantities $\langle x_i-x_{i0}\rangle$ and $\langle y_i-y_{i0}\rangle$ were determined for each 2000 particles added. Here x_i and y_i are the coordinates of the ith particle. x_{i0} and y_{i0} are the coordinates of the first particle to be added to the tree containing the ith particle (i.e., the coordinates of the root of the tree). For each group of 2000 particles the quantity R given by

$$R=\langle y_i-y_{i0}\rangle/\langle x_i-x_{i0}\rangle \tag{4}$$

was determined. Typical results for an angle of incidence of 80° are shown in Fig. 4. Note that R approaches a constant for large deposits and its value, $\bar{R}$, estimated by averaging over the last 100 000 particles added. The angle of growth for the trees (which can be identified with the angle of growth for the columns at large angles of incidence is given by

$$\beta'=\tan^{-1}[(\bar{R})^{-1}]\ . \tag{5}$$

We have also measured a second angle using the quantity

$$S=\langle y_i-y_{is}\rangle/\langle x_i-x_{is}\rangle\ , \tag{6}$$

where x_{is} and y_{is} are the coordinates of the particle in the deposit to which the ith particle becomes attached. The angle given by

$$\theta=\tan^{-1}[(\bar{S})^{-1}] \tag{7}$$

is called the angle of attachment.

Table I shows the results obtained for both these angles

TABLE I. Some results obtained from two-dimensional simulations of ballistic deposition with a constant angle of incidence.

Angle of incidence (α) (deg)	Mean angle of tree growth (β) (deg)	Tangent rule prediction (deg)	$\alpha-\beta$ (deg)	Mean angle of attachment (deg)
10	11.55	5.04	−1.55	9.11
20	16.17	10.31	3.83	18.67
30	23.94	16.10	6.06	27.90
40	31.02	22.76	8.98	36.92
50	39.46	30.79	10.54	46.72
55	43.91	35.53	11.09	51.16
60	47.13	40.89	12.87	55.65
65	51.24	47.00	13.76	60.33
70	55.46	53.95	14.54	65.53
75	59.44	61.81	15.56	69.74
80	63.93	70.57	16.07	74.36
85	69.00	80.08	16.00	79.98
87.5	71.47	85.0	16.03	82.53

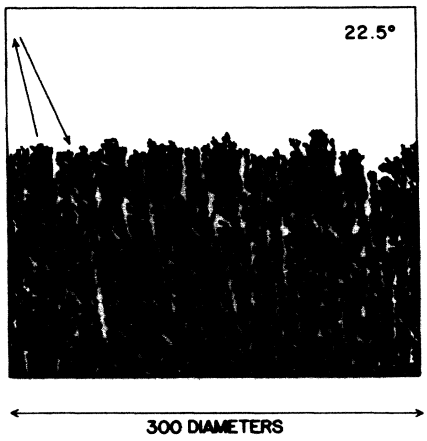

FIG. 5. Results of a small-scale off-lattice simulation of 2D ballistic deposition with an angle of incidence (inward pointing arrow) of 22.5°. Direction of growth predicted by the tangent rule is indicated by the outward pointing arrow.

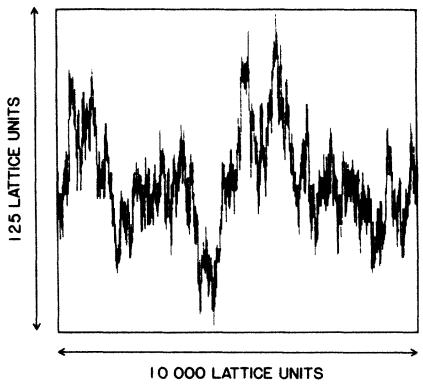

FIG. 6. Section from the surface of a 2D square-lattice deposit grown to a height of 5000 lattice units on a base 2^{18} lattice units long.

for various angles of incidence. At large angles of incidence, where the definition of the direction of columnar growth is unambiguous and coincides with the direction of tree growth, the deviation from the tangent rule is quite strong. A better empirical rule seems to be

$$\alpha-\beta=C\ , \tag{8}$$

where C is a constant angle of approximately 16°. At smaller angles of incidence the definition of the angle of growth becomes quite ambiguous and there seem to be two angles which can be associated with the morphology (Fig. 5). We have tried (so far unsuccessfully) to develop (nonvisual) methods that determine the angle of growth at small angles of incidence. In any event our results indicate that 2D simulations of ballistic deposition are not consistent with the tangent rule. Although we have not carried out 3D off-lattice simulations it seems most probable that similar results will be found. Consequently, we conclude that the success of the tangent rule in predicting the morphology of a large range of real systems cannot be explained in terms of simple models for ballistic deposition. It also seems most probable that the tangent rule is not a universal rule for vapor-deposition processes.

B. Scaling of the interface for 2D square lattice simulations

In order to estimate values for the exponents α and γ [Eq. (3)], simulations were carried out on a square lattice with particles sticking at nearest-neighbor positions only. The exponent ν was first obtained using very wide strips (2^{18} sites long) on which particles were deposited until a mean height ($\bar{h}$) of 5000 lattice units was reached.

At this stage each deposit contains about 6×10^8 occupied sites. Figure 6 shows a section taken from the surface of one of these deposits. Unlike real surfaces generated by ballistic deposition which look like the head of a cauliflower and have a noticeable anisotropy, the surface shown in Fig. 6 does not appear to be anisotropic. However, we have not made a quantitative study of this aspect of the surface structure.

For active zones with a mean height in the range $50\le\bar{h}\le500$ lattice units we find that the exponent ν has an effective value of 0.331 ± 0.006 and for active zone heights in the range $500\le\bar{h}\le5000$ we find $\nu=0.308\pm0.011$. The range of uncertainty given here and elsewhere in this paper represents the 95% confidence limit. The value obtained for ν is in good agreement with the result obtained by Family and Vicsek[27] (0.30 ± 0.2) from smaller-scale simulations and is also in good agreement with the results obtained by Meakin, Jullien, and Botet[30] ($\nu=0.307\pm0.007$) from large-scale simulations using version C of the Eden model.[28] Since the structure generated by ballistic models is uniform on all but short-length scales, we have $M\sim\bar{h}$ and Eq. (3) can be rewritten as

$$\xi\sim l^{\alpha'}f(M/l^{\gamma'})\ , \tag{9}$$

where M is the deposit mass (number of occupied sites). If the argument of the scaling function, $f(x)$, is small we expect to find $f(x)\sim x^{\nu'}$ with $\nu'=\alpha'/\gamma'$. Since $\bar{h}\sim M$ we expect that $\alpha'=\alpha$, $\gamma'=\gamma$, and $\nu'=\nu$. A direct measurement of the effective value of ν' from the dependence of ξ on M gives $\nu'=0.307\pm0.013$ for $6\times10^7\le M\le6\times10^8$ and $\nu'=0.335\pm0.006$ for $6\times10^6\le M\le6\times10^7$ deposited sites.

To obtain an estimate for the value of the exponent α, Eq. (3), deposits have been grown on strips of width l ($l=16$–2048 lattice units). For $l<512$ deposits have been grown to a height much greater than l^{γ} (a conservative estimate of $\frac{5}{3}$ for the value of γ was used) and the dependence of the width of the active zone, ξ, on l was determined only for deposit heights greater than $20l^{\gamma}$. For $l=1024$ and 2048 this procedure was not possible and the width of the active zone (ξ_0) was determined by fitting the dependence of ξ on M by a function of the form

$$\xi=\xi_0(1+AM^{-w})\ . \tag{10}$$

In this equation ξ is the measured width of the active zone and ξ_0 is the asymptotic ($M\to\infty$) value for the width of the active zone if Eq. (10) correctly represents

TABLE II. Width of the active zone (ξ_0) in the limit $h \gg l^\gamma$ for strips of width l. The results shown in this table were obtained on a square lattice for the NN model.

l	ξ_0
8	0.236 81±0.000 16
16	1.9796±0.0006
32	2.8878±0.0016
64	4.061±0.005
128	5.652±0.015
256	7.83±0.05
512	10.85±0.20
1024	14.84±0.15
2048	21.28

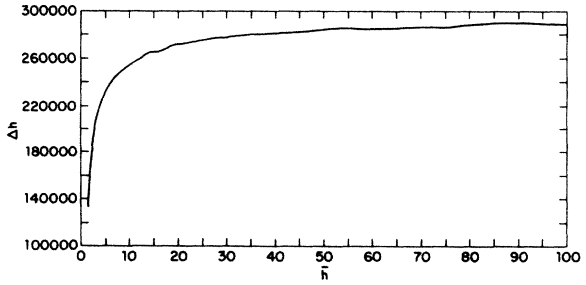

FIG. 8. Dependence of the sum of the step heights (ΔH) on the mean surface height ($\bar{h}$) for a 2D square-lattice simulation carried out using the NN model with a base 2^{18}(262 144) lattice units wide.

the form of the finite-size correction. For $l=1024$ the results from six deposits ($M=8\times10^8$, 8×10^8, 3×10^9, 3×10^9, 3.75×10^9, and 4.4×10^9) were used and for $l=2048$ the results from four deposits ($M=8\times10^8$, 2.8×10^9, 3.2×10^9, and 4×10^9) were used. Table II shows the dependence of the width of the active zone (ξ_0) on l.

The dependence of the width of the active zone (ξ_0) on the strip width (l) is shown in Figs. 7(a) and 7(b). In Fig. 7(a) the results of an attempt to fit the dependence of $\ln(\xi_0)$ on $\ln(l)$ using a straight line (with a ruler) is shown

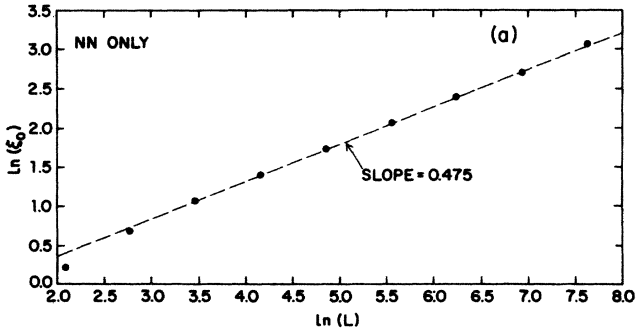

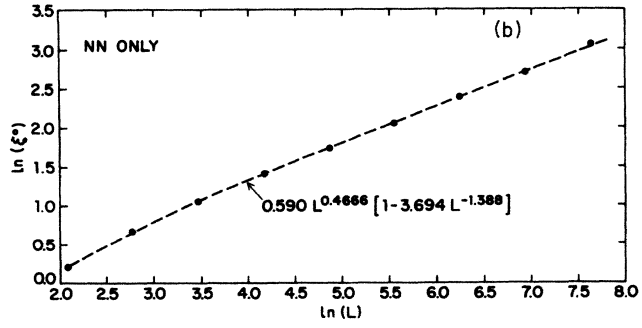

FIG. 7. (a) Dependence of the saturated ($\bar{h}\to\infty$) width of the active zone (ξ_0) on the strip width l from 2D simulation of ballistic deposition on a square lattice. (b) Result of an attempt to fit this dependence by a function of the form $\xi_0=Al^\mu(1+Bl^{\mu'})$.

and in Fig. 7(b) the results of a nonlinear least-squares fitting to a function of the form

$$\xi_0=al^\mu(1+Bl^{\mu'}) \tag{11}$$

is shown. Taken together these results indicate that the asymptotic dependence of ξ_0 on l can be expressed as $\xi_0\sim l^\alpha$ where the exponent α has a value of about 0.47. This value is much closer to the theoretical value[32] of 0.5 than the result $\alpha=0.42\pm0.03$ obtained by Family and Vicsek.

A quantity which is of interest in understanding the nature of the surface of ballistic aggregates is the distribution of step heights, δh, in the active zone, where $\delta h_i=|h_i-h_{i+1}|$. In Fig. 8 we consider the sum of the step heights (ΔH) defined by

$$\Delta H=\sum_{i=1}^{l}\delta h_i\ . \tag{12}$$

The length of the interface in an L' metric is $\Delta H+l$. This quantity might depend on the mean height of the active zone ($\bar{h}$) given by

$$\bar{h}=\left[\sum_{i=1}^{l}h_i\right]\Big/l\ . \tag{13}$$

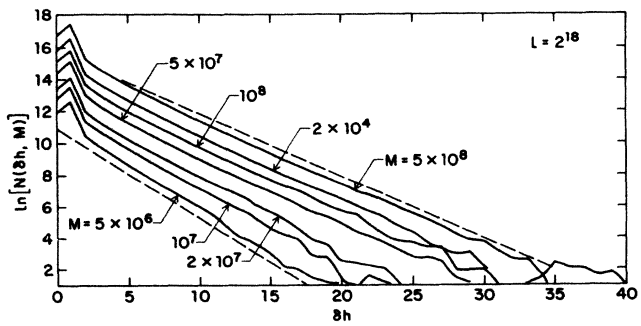

FIG. 9. Distribution of step heights, $N(\delta h,M)$, for 2D square-lattice deposits of various masses, M, grown using the NN model using a substrate 2^{18} lattice units long.

TABLE III. Dependence of the width of the active zone (ξ_0) on the strip width (l) in the limit $\bar{h} \gg l^{5/3}$ for the NNN model.

l	ξ_0
8	1.840 96±0.000 46
16	3.1411±0.0009
32	4.6354±0.0023
64	6.4727±0.0068
128	8.860±0.024
256	12.148±0.042
512	16.609±0.070
1024	22.40
2048	30.69

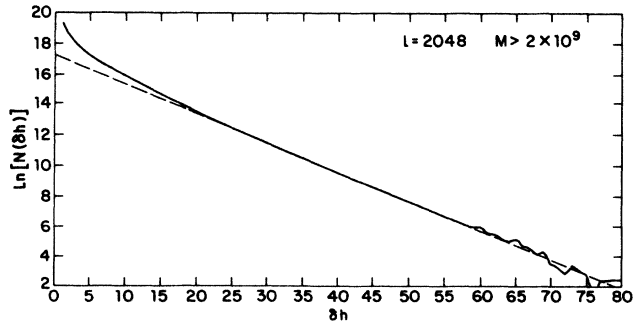

FIG. 10. Limiting ($\bar{h} \to \infty$) step height distribution obtained from 2D simulations carried out on a square-lattice strip 2048 lattice units wide using the NNN model.

The results shown in Fig. 8 are from a single simulation with a strip width (l) of 2^{18}. They show that ΔH at first increases rapidly with increasing deposit thickness ($\bar{h}$) but soon approaches a limiting value. Least-squares fitting straight lines to the dependence of $\ln(\Delta H)$ on $\ln(\bar{h})$ for deposit heights in the range $500 \leq \bar{h} \leq 5000$ lattice units for five simulations gives a value for the effective exponent η, defined by

$$\Delta H \sim \bar{h}^{\eta} , \tag{14}$$

of 0.002 78±0.000 24 indicating that ΔH becomes independent of $\bar{h}$. For deposit heights in the range 2500–5000 lattice units $\Delta H/l$ has the value of 1.136 00±0.000 05. Thus the length of the interface does not grow with $\bar{h}$ and is proportional to l.

We have also determined the distribution of step sizes at various stages during the deposition process. Figure 9 shows these distributions. In this figure $N(\delta h,M)$ is the number of steps of height δh obtained for deposit masses in a small range $(M+\delta M)$ of masses (δM is about $0.025M$). It is apparent from this figure that the dependence of $N(\delta h,M)$ on δh can be expressed as

$$N(\delta h,M) \simeq Ae^{-k\delta h} , \tag{15}$$

and as the deposit mass increases the constant k decreases but the distribution retains its exponentially decaying form and the decay constant (k) seems to be approaching a constant value of about 0.39. This indicates that large steps are (exponentially) improbable and that the surface of the ballistic aggregate is not a self-similar fractal.

A similar equally extensive set of simulations were carried out using a modified version of square-lattice ballistic aggregation in which particles were allowed to stick if they were on unoccupied sites which were either nearest neighbors or next-nearest neighbors to occupied sites. This NNN model gives structures which have a lower density than the NN model described above (0.2469 for the NNN model versus 0.4684 for the NN model). However, the structures generated by both of these models are very similar and the results for the NN and the NNN models are summarized in Tables II, III, and IV.

Tables II and III show the dependence of the width of the active zone (in the limit $\bar{h} \gg l^{5/3}$) on the strip width l. Table IV compares the exponents which describe the structure of the active zone for both the NN and the NNN square-lattice ballistic-deposition models.

For both the NN and the NNN models the distribution of step heights was determined in the limits $\bar{h} \ll l$ (Fig. 9, for example) and $\bar{h} \gg l^{5/3}$. Figure 10 shows some results obtained for the NNN model with a strip width of 2048 lattice units. 2×10^9 sites were added before the step size distribution $N(\delta h)$ was determined and was measured as the next 1.2×10^9 sites were added. Except for small step heights (δh) our results again strongly suggest an exponential distribution for step sizes which, in this case, can be expressed as

$$N(\delta h) = Ae^{-k\delta h} \quad (k \simeq 0.192) . \tag{16}$$

This is similar to the results obtained for the NN model.

TABLE IV. Effective values for the exponents which describe the structure and growth of the active zone for the NN and NNN models for square-lattice ballistic deposition.

Exponent	Range	NN	NNN
ν	$0.01h_{\max} \leq \bar{h} \leq 0.1h_{\max}$	0.331±0.006	0.323±0.004
ν	$0.1h_{\max} \leq \bar{h} \leq h_{\max}$	0.308±0.011	0.309±0.011
α		0.47±0.01	0.45±0.01
α	$32 \leq l \leq 2048$	0.476±0.003	0.452±0.003
α	Nonlinear fit	0.467	0.445
η	$0.1h_{\max} \leq \bar{h} \leq h_{\max}$	0.002 78±0.000 24	0.003 66±0.000 33
$\gamma=\alpha/\nu$	$0.1h_{\max} \leq \bar{h} \leq h_{\max}$	1.50±0.1	1.45±0.1

C. Discussion of 2D simulation results

The foregoing results on step size distribution are rather unexpected. As we have remarked, there are a very small number of large steps. The surface cannot be a self-similar fractal. In fact, we will prove a stronger result: The asymptotic value of the length of the surface is proportional to l.

The proof of this bound on the length of the interface is simple, if, as proved for ballistic aggregation,[10] the density of the aggregate does not indefinitely decrease. The essence of the argument is that if a particle is deposited on the edge of a step of height δh, then the mean height of the interface $\bar{h}$ increases by $\delta h/l$ where l is the width of the sample. Thus if n is the number of particles deposited per unit of substrate and ρ is the density of the deposit we have

$$\frac{1}{\rho}=\frac{\partial \bar{h}}{\partial n}\sim\langle \delta h\rangle , \tag{17}$$

where $\langle \delta h\rangle=\Delta H/l$ is a uniform average over the interface. Of course, $l(\langle \delta h\rangle+1)$ is the length of the surface, as above. A rigorous analysis (see Appendix) gives for the $d=2$ NN model:

$$\frac{1}{\rho}-1\le\langle \delta h\rangle\le\frac{2}{\rho} , \tag{18}$$

but the argument should hold in any space dimension.

One can also present a simple argument for the distribution of step heights δh as follows. Qualitatively each step can do two things: it can grow in height by accreting a particle on top of itself and it can advance in the direction it faces by accreting a particle on its leading edge. The latter process necessarily entails collision with another step (albeit perhaps of zero height). Since opposite facing steps approach each other systematically whereas similar facing steps have only a diffusive relative motion, we will focus on collisions of the former pairs. We introduce the notation $P_R(\delta h),P_L(\delta h)$ for the statistical distributions of left and right facing steps (which should in fact be equal). Then we have the equations of motion:

$$\frac{\partial}{\partial n}P_R(x)=\frac{\partial}{\partial x}P_R-2P_R(x)\sum_y P_L(y)+2\sum_y P_R(x+y)P_L(y) , \tag{19}$$

and symmetrically for $P_L(x)$. The terms are, respectively: increase of δh, loss by collision, and gain by collision with a larger step. For a steady state with $P_R=P_L=P/2$ we then have in a continuum approximation:

$$-2\frac{\partial}{\partial x}P(x)-2P(x)+2\int_0^\infty dy\,P(x+y)P(y)=0 , \tag{20}$$

which has an exponential solution $P(x)=ke^{-kx}$ with $k=\frac{1}{2}$. The value of k compares fortuitously well with the observed limiting slope of Fig. 9, $k_{\rm obs}\sim 0.39$ for the NN model. Thus we have good evidence both from simulation and analysis that small steps dominate the fluctuations in height. This fact leads us to suspect that the single-step model should be essentially identical to true ballistic aggregation. We now turn to a discussion of simulation results for the single-step case.

TABLE V. Dependence of the width of the active zone (ξ_0) in the limit $\bar{h}\gg l^{5/3}$ on the strip width (l) for the single-step ballistic-deposition model.

l	ξ_0
8	0.806 20±0.000 025
16	1.135 61±0.000 12
32	1.614±0.004
64	2.2957±0.0017
128	3.254±0.004
256	4.608±0.019
512	6.490±0.037
1024	9.065±0.015

D. Single-step model in 2D

A similar set of simulations to those discussed above has been carried out for the single-step model in 2D. Double sites were added to a line 2^{18} (262 144 sites) wide until the deposit grew to a height of 5000 lattice sites (i.e., until about 6.5×10^8 double sites had been added). In this model, the density of the deposit is 1.0. From 15 simulations the result $\nu=0.332\pm0.003$ was obtained for the active zone of deposits which had grown to heights in the range $0.01h_{\rm max}\le\bar{h}\le0.1h_{\rm max}$. For deposits with heights in the range $0.1h_{\rm max}\le\bar{h}\le h_{\rm max}$ the result was $\nu=0.330\pm0.012$. These results suggest that the asymptotic value for the exponent may be exactly $\frac{1}{3}$ for this model. We have also determined the dependence of the width of the active zone, ξ, on the strip width l for strips of width 8–1024 lattice units. The results of these simulations are shown in Table V. For this model, the dependence of $\ln(\xi_0)$ on $\ln(l)$ is almost perfectly linear and the effective value for the exponent α is 0.5029 ± 0.0009 for $8\le l\le1024$, 0.500 ± 0.0015 for $64\le l\le1024$, and 0.504 ± 0.0024 for $8\le l\le64$ lattice units. These results strongly suggest that the limiting value for the exponent α may be exactly $\frac{1}{2}$ for this model. We conclude that $\nu\simeq\frac{1}{3}$, $\alpha\simeq\frac{1}{2}$, and $\gamma\simeq\frac{3}{2}$ for the single-step model.

E. Three-dimensional ballistic deposition

Simulations of ballistic deposition were carried out on a 3D cubic lattice with periodic boundary conditions in the lateral directions. In this model the adjacent sites at which particle sticking occurs are unoccupied sites with one or more occupied nearest neighbors. The surfaces on which the deposition process was simulated were of size $l\times l$ lattice units with $l=8$, 16, 32, 64, 128, 256, 512, and 1024. For surfaces in the size range 8×8–512×512 the deposition process was carried out until the mean height of the active zone had reached heights which were very much greater than l^γ. For the case $l=512$ more than 5×10^9 sites were deposited. Table VI shows the dependence of the width of the active zone (ξ_0) on $\ln(l)$ and sug-

TABLE VI. Dependence of the saturated width of the active zone (ξ_0) obtained from 3D simulations of ballistic deposition onto $l \times l$ surfaces using a cubic lattice model with nearest-neighbor sticking.

l	ξ_0
8	1.4557±0.0007
16	1.9895±0.0036
32	2.5540±0.0058
64	3.250±0.016
128	4.080±0.029
256	5.227±0.040
512	6.476±0.020

gests that the asymptotic value for the exponent α [Eq. (3)] may be close to $\frac{1}{3}$. We have also measured the dependence of the width of the active zone (ξ) on the mean height of the active zone using simulations carried out on a 1024×1024 surface. Figure 11(b) shows the results obtained from this simulation which suggests that the exponent ν may have a value close to $\frac{1}{4}$. However, in this case, it is difficult to approach the limit $\bar{h} \ll l^{\gamma}$ and still be at heights which are sufficiently large to see the correct asymptotic behavior (i.e., we need to satisfy $\bar{h} \gg 1$ and $\bar{h} \ll l^{\gamma}$ simultaneously).

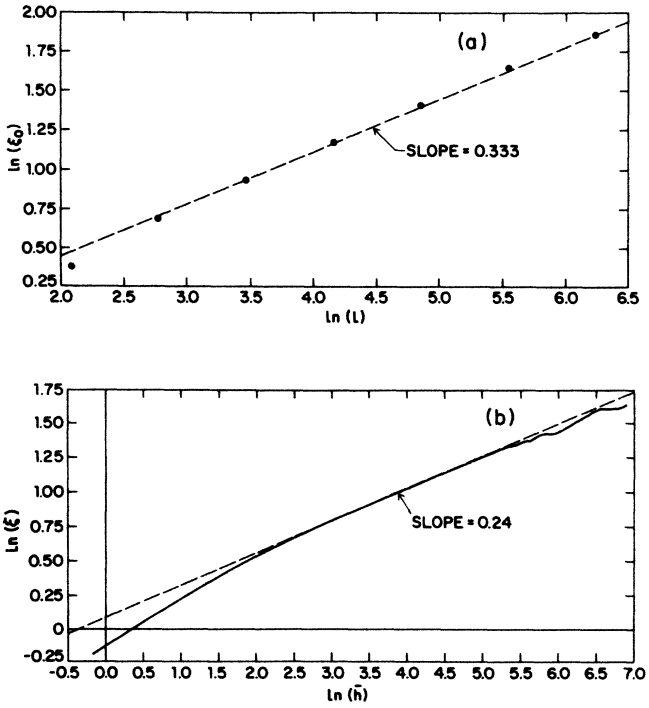

FIG. 11. (a) Dependence of the saturated width of the active zone (ξ_0) on the substrate size ($l \times l$) obtained from 3D cubic lattice simulations using the NN model. (b) Shows how the width of the active zone (ξ) depends on the mean height of the active zone ($\bar{h}$) for a simulation carried out on a base of 1024×1024 lattice units.

F. Three-dimensional single-step model

A three-dimensional version of the single-step model described above was also investigated. In this model (illustrated in Fig. 12) we start with a checkerboard of raised and lowered sites [Fig. 12(a)]. Positions on the $l \times l$ surface are selected randomly and the height at these positions is raised by two lattice units if all four nearest neighbors have a height which is greater than that of the selected site. Simulations were carried out on $l \times l \times h$ simple cubic lattices with $l = 8$, 16, 32, 64, 128, 256, and 512. For the case $l = 512$ lattice units, a total of 2×10^9 pairs of sites were added ($\bar{h} \simeq 1.6 \times 10^4 \simeq 4l^{4/3}$). For smaller values of l the limit $\bar{h} \gg l^{\gamma}$ was approached more closely. These simulations gave results which were very similar to those obtained from the ordinary 3D ballistic deposition model [Fig. 11(a)] and a value of 0.363±0.005 was obtained for the exponent α.

Simulations were also carried out using 1024×1024 surfaces. In this case, we cannot approach the limit $h \gg l^{\gamma}$ and these simulations were used to investigate the dependence of the surface height variance ξ on the mean surface height $\bar{h}$. Five simulations were carried out in which deposits were grown to a height of 1000 lattice units. Again, the results obtained were very similar to those for the 3D NN model [Fig. 11(b)] and an exponent ν with a value of about $\frac{1}{4}$ was obtained assuming that the dependence of ξ on $\bar{h}$ is described by Eq. (3). For mean heights in the range $5 \leq \bar{h} \leq 50$ lattice units ν has an effective value of 0.221±0.003 and for $50 \leq \nu \leq 500$ lattice units $\bar{h} = 0.2303 \pm 0.0006$. These uncertainties are stan-

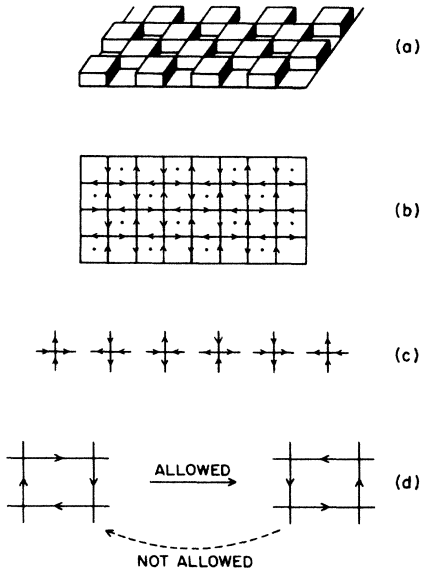

FIG. 12. (a) Initial configuration of the surface of the single-step model in 3D. (b) Mapping of the surface to a vertex configuration. (c) Six allowed vertices. (d) Allowed transitions of a plaquette.

dard errors obtained from the least-square-fitting procedure. The true statistical uncertainties are substantially larger and systematic errors are probably even more important. In three-dimensional simulations it is particularly difficult to satisfy simultaneously the conditions $\bar{h} \ll l^{\gamma}$ and $\bar{h} \gg 1$.

G. Analytic results for single-step models

Since the single-step models both in 2D and 3D have similar scaling behavior to full ballistic aggregation, we are motivated to devise analytical treatments for these simpler processes. In the process we will produce an almost trivial proof that $\alpha = \frac{1}{2}$ in 2D in agreement with simulations and Ref. 32. We will show in the next section that there is a relationship between α and γ, so that we can give a full treatment in this case.

The single-step model in 2D can be mapped onto a spin model with an up-spin representing a step up in the interface and down-spin a step down, see Fig. 13. Growth at a site is represented by a biased nearest-neighbor spin exchange with an up-spin moving only to the left and a down-spin to the right. The opposite sense of spin exchange would correspond to a lowering of height which we do not allow. The interface dynamics in the moving frame $\bar{h}=0$ is now a spin exchange problem. The height at site m is given by

$$h_m = \sum_{i=1}^{m} \sigma_i + h_1 , \tag{21}$$

where $\sigma_i = \pm 1$. Also $\sum \sigma_{\uparrow} = \sum \sigma_{\downarrow}$ follows from periodic boundary conditions. Now suppose that after many spin exchanges the system approaches the equilibrium of the spin model. In this "long-time" limit we would have

$$\langle \sigma_i \sigma_j \rangle = \delta_{ij} . \tag{22}$$

Then we have from Eq. (21):

$$\langle (h_m - h_n)^2 \rangle = | m - n | . \tag{23}$$

This is the definition of a self-affine fractal[7,34,35] with a fractal dimension of $\frac{3}{2}$. Also, it follows at once that

$$\xi^2 = \langle (h_m - \bar{h})^2 \rangle \sim l , \tag{24}$$

so that $\alpha = \frac{1}{2}$. Now, we can show that the spin system maintains equilibrium, where every configuration such that the magnetization is zero is equally likely from the following observations.

(a) Every configuration can be formed by one deposition in one way for each maximum of its interface.

(b) Every configuration can form, by one deposition, one new configuration for each minimum of its interface.

(c) The number of minima and maxima are always equal.

It follows that if every allowed configuration is equally likely, then every configuration is as likely to be formed as lost, and equilibrium preserves itself.

In 3D the single-step interface can be mapped onto the six-vertex model with equal vertex energies; see Fig. 12. The initial configuration [Fig. 12(a)] is mapped onto the vertex configuration Fig. 12(b). Looking down on a vertex and sweeping close around it anticlockwise, a step-up is denoted by outwards arrow and a step-down by an inwards arrow. The allowed vertices are those with equal numbers of incoming and outgoing arrows, as shown in Fig. 12(c). Thus the arrows constitute a conserved current, and it is easy to see that the difference in height between two sites is the net transverse current flowing across a line between them. The allowed growth step is to reverse all the arrows of a local cycle (plaquette) from clockwise to anticlockwise (but not vice versa), as shown in Fig. 12(d) and may be viewed as a simultaneous horizontal and vertical biased spin exchange each as in the 2D case. The height at site n,m is

$$h(n,m) = \sum_{i=1}^{n} \sigma^{v}_{i,1} + \sum_{j=1}^{m} \sigma^{h}_{n,j} + h(1,1) , \tag{25}$$

where σ^v and σ^h are the vertical and horizontal arrows with values ± 1. Once more, if we know the equilibrium arrow correlation function, we can calculate α.

Finding the equilibrium of this vertex model is not as easy as the 2D case. We should note that the ways of forming a configuration are in correspondence with the maxima of its interface (anticlockwise plaquettes) and the ways it can grow with the minima (clockwise plaquettes) as before. Thus if the ensemble of all possible configurations (equally weighted) has predominantly nearly equal number of maxima and minima, then at long times our system probably reaches a good approximation to the equilibrium of our 3D model. Since maxima and minima are features of the local geometry, this assumption is likely to be justified in the limit of a large system.

If we do assume that all configurations of the vertex model are equally likely, then using the result of Sutherland[36] for the arrow correlation in the six-vertex model, we obtain the result of Beijeren[37] for the body-centered solid-on-solid model in the limit of infinite temperature

$$\langle (h_a - h_b)^2 \rangle \sim \ln(R_{ab}) , \tag{26}$$

where R_{ab} is the distance between sites a and b. The result is also obtained for the discrete Gaussian model[38] which we believe to be in the same universality class. We can understand this equation by noting that the long wave-vector components of a conserved "current" density are correlated. In fact, if all allowed current configurations are equally likely the correlation function in real

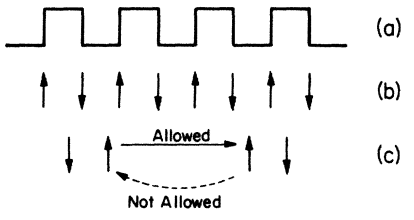

FIG. 13. (a) Initial configuration of the surface of the single-step model in 2D. (b) Mapping of the surface to a spin configuration. (c) Allowed spin exchanges.

space is

$$\langle j(0)j(r)\rangle \sim 1/r^2 , \tag{27}$$

which is also the arrow correlation result of Sutherland.[36] This logarithmic law corresponds conceptually to $\alpha=0$ and is rather difficult to test; we have seen that our data does not support it.

Kardar *et al.*[32] obtain $\alpha=\frac{1}{2}$ for this case as in 2D. Their result is different from ours ($\alpha=0$) *and* from the simulation data ($\alpha\approx\frac{1}{3}$). We have no explanation of this multiple discrepancy.

H. Continuum approximation and scaling

With both simulation and theory suggesting universality for the asymptotic scaling of the interface thickness (at least in $d=2$) it is natural to look for simplified equations of its motion on the large scale. The observed exponents ν and α are less than unity. Thus $\xi/l, \xi/\bar{h}\to 0$ as $\xi\to\infty$ so that coarse scale derivatives dh/dx exist, and the proof that the step heights are bounded shows that dh/dx still exists even locally. Thus we are led to consider differential equations. For the NN model we have a growth rate, averaged over temporal noise, given by

$$\left\langle \frac{\partial h}{\partial n}\right\rangle = \langle \delta h\rangle_{\rm LSA} \sim \langle \delta h\rangle_0 (1+\epsilon\,|\nabla h\,|^2\cdots) , \tag{28}$$

where $\langle\ \rangle_{\rm LSA}$ is the local spatial average $\epsilon\,|\nabla h\,|^2$ is the first term in a gradient expansion.

For the single-step model we have

$$\left\langle \frac{\partial h}{\partial t}\right\rangle = \prod_{i=1}^{d-1} c_{\downarrow}^i c_{\uparrow}^i , \tag{29}$$

where i ranges over the $d-1$ types of links in the substrate lattice and $c_{\downarrow}^i$ ($c_{\uparrow}^i$) is the local probability for such a link to be downwards (upwards); we have assumed the links to be uncorrelated locally. We also have

$$c_{\downarrow}^i + c_{\uparrow}^i = 1, \quad i=1,2,\ldots,d-1 , \tag{30}$$

$$\frac{\partial h}{\partial x_i} = c_{\downarrow}^i - c_{\uparrow}^i , \tag{31}$$

giving

$$\left\langle \frac{dh}{dt}\right\rangle = \prod_{i=1}^{d-1}\left\{\frac{1}{4}\left[-\left[\frac{\partial h}{\partial x_i}\right]^2\right]\right\}$$

$$\sim 4^{1-d}(1-|\nabla h\,|^2+\cdots) , \tag{32}$$

where the last expansion is in the small gradient limit. Subtracting the advance of a flat interface, both equations can be rescaled in the weak gradient limit to give the form considered by Kardar *et al.*,[32]

$$\frac{\partial \tilde{h}}{\partial t} \sim (\nabla\tilde{h})^2 + \eta(\mathbf{x},t) . \tag{33}$$

where the noise $\eta(\mathbf{x},t)$ is such that $\langle\eta(\mathbf{x},t)\rangle=0$ and

$$\langle\eta(\mathbf{x},t)\eta(\mathbf{x}',t')\rangle = 2D\delta^d(\mathbf{x}-\mathbf{x}')\delta(t-t') .$$

Here we observe that if for large-scale solutions we can neglect the noise, then there only exist nontrivial solutions to the above with the scaling form

$$\tilde{h}(\mathbf{x},t) = t^{\nu} f(\mathbf{x}t^{-\nu/\alpha}) \tag{34}$$

if

$$\frac{2}{\alpha} = 1+\frac{1}{\nu} , \tag{35}$$

whereupon $f(\mathbf{y})$ obeys

$$\nu f(\mathbf{y}) - \frac{\nu}{\alpha}\mathbf{y}\cdot\frac{\partial}{\partial y} f(\mathbf{y}) = \left[\frac{\partial}{\partial y} f(\mathbf{y})\right]^2 . \tag{36}$$

This scaling law is consistent in two dimensions with the results of Kardar *et al.*[32] and our simulation data. For the single-step model in $d=2$ where we have $\alpha=\frac{1}{2}$ explicitly, it determines $\nu=\frac{1}{3}$.

For the single-step model in $d=3$, where we have presented an argument that $\alpha\to 0$, it follows that $\nu\to 0$ also. However, $\gamma=\alpha/\nu$, the crossover exponent should approach $\gamma=2$. This may ultimately be the clearest prediction to test in this case.

IV. DISCUSSION

In our analysis of the lattice models for ballistic deposition we have assumed that the scaling form found by Family and Vicsek is correct and have attempted to measure the exponents α, ν, and γ by approaching as close as possible to the asymptotic limits available to us. To determine the exponent ν we require $l^{\gamma}\gg\bar{h}$ and $\bar{h}\gg 1$ and to determine α we require $\bar{h}\gg l^{5/3}$ and $l\gg 1$. Clearly, very large-scale simulations are needed to satisfy these conditions. Despite the fact that we have grown very large deposits (in some cases deposits containing more than 10^9 occupied sites) it is clear we have not reached the asymptotic limits and that the values we have obtained for the effective exponents α, ν, and γ should be regarded as *estimates*. In the case of the single-step model the corrections to the simple scaling picture are very much smaller and we believe that our results for this model are quite accurate. In any event, our results from all of the 2D models are consistent with the theoretical work we have presented and that of Kardar *et al.*[32] ($\alpha=\frac{1}{2}$, $\nu=\frac{1}{3}$, $\gamma=1.5$). However, for both the NN and the NNN 2D ballistic deposition model the exponent α is smaller than $\frac{1}{2}$ and seems to be decreasing with increasing l. It would be desirable to carry out simulations with larger values of l but this does not seem to be practical since much larger scale simulations would be needed to approach the asymptotic limit and even for the largest-scale simulations the statistical uncertainties become larger with increasing l (see Tables II, III, and IV).

In this case of the three-dimensional NN model and the single-step model our results suggest that $\alpha\simeq\frac{1}{3}$ and $\nu\simeq\frac{1}{4}$. However, in three dimensions it is even more difficult to approach the asymptotic limits in which we expect to find the simple behavior

$$\xi\sim\bar{h}^{\nu} \text{ for } \bar{h}\gg 1 \text{ and } \bar{h}\ll l^{\gamma} , \tag{37}$$

$$\xi\sim l^{\alpha} \text{ for } \bar{h}\gg l^{\gamma} \text{ and } l\gg 1 . \tag{38}$$

Our observation that the distribution of step heights, $N(\delta h)$, in the ballistic-deposition models is an exponentially decaying function of δh indicates that the surface of 2D ballistic deposits is not a self-similar fractal. The fact that large steps are exponentially improbable for the square-lattice ballistic-deposition models strongly suggests that these models and the single-step model should belong to the same universality class. If this is the case we expect to find $\alpha=\frac{1}{2}$ and $\nu=\frac{1}{3}$ for 2D ballistic deposition. Results we have obtained for 2D square-lattice ballistic-deposition models are very similar to those found in 2D Eden models carried out in a similar manner on about the same scale.[30] This supports the idea that both the Eden model and the ballistic-deposition model belong to the same universality class ($D_e=D_b=d$, $\alpha_e=\alpha_b=\frac{1}{2}$, $\nu_e=\nu_b=\frac{1}{3}$). In the case of the Eden model, Plischke and Racz have measured the exponent γ from the dynamics of the "normal modes" which describe the evolution of the surface. Using a strip geometry like that employed for the ballistic-deposition simulations described above they find $\gamma=1.55\pm0.15$ in good agreement with other measurements of γ for Eden models[28-30] and our indirect determination of γ ($\gamma=\alpha/\nu$) for the ballistic-deposition models. For the NN model we find $\gamma=1.50\pm0.1$ and for the NNN, $\gamma=1.45\pm0.01$. For 3D the situation is much less clear. Neither our analysis nor that of Ref. 32 agrees with our direct simulations. Further work on this case (which is, after all, the one of most direct physical interest) is needed.

Our results for the dependence of the angle of growth on the angle of incidence for 2D off-lattice ballistic deposition indicates that the well-known "tangent rule" is not quantitatively accurate. Nevertheless, the tangent rule appears to be a useful empirical rule which summarizes approximately the behavior observed in a variety of real systems. Our simulation results suggest that for large angles of incidence (α) the angle of growth (β) is related to α by

$$\beta=\alpha-C\ , \tag{19'}$$

where the angle C has a value of about 16°. This angle is not much different from the limiting fan angle for deposition onto a single particle (18.3 ± 1.5°) (Ref. 23) obtained from off-lattice computer simulations. Indeed for grazing incidence ($\alpha=90$°) we expect that the angle of growth should be given by

$$\beta=\alpha-\theta \tag{20'}$$

where θ is the limiting fan angle.

Note added in proof. In this paper we have consistently used the width of the active zone to define α and ν. One could also use the variance of the height itself. In 2D this scheme leads to a slower approach to the same asymptotic values ($\alpha=0.5$ and $\nu=0.33$). In 3D the apparent exponents are smaller than what we have quoted here. This will be the subject of further work.

ACKNOWLEDGMENTS

P.R. and L.M.S. are supported by U.S. Department of Energy Grant No. DE-FG02-85ER45189. We would like to thank M. Kardar for a useful discussion.

APPENDIX

We show that the length of the interface of a ballistic deposit; $\sum_n(1+|h_n-h_{n-1}|)$ is not characteristic of a self-similar fractal, but is proportional to l, the width. This is achieved by showing that the mass per unit substrate,

$$\mu=\langle 1+|h_n-h_{n-1}|\rangle\ , \tag{A1}$$

lies within bounds of the reciprocal density of deposition,

$$\rho^{-1}=\langle \max(h_{n+1}-h_n,h_{n-1},h_n,1)\rangle\ . \tag{A2}$$

Note that this is just the average increase in column height per deposition on the substrate. Defining $\delta_n=h_n-h_{n-1}$, $s_n=|\delta_n|$, and $t_n=\max[\delta_{n+1},-\delta_n,1]$, we have

$$\mu=\langle 1+s_n\rangle\ , \tag{A3}$$

$$\rho^{-1}=\langle t_n\rangle\ , \tag{A4}$$

where $s_n=t_n$ if and only if $s_n>s_{n+1}$. Defining

$$s_n'=\begin{cases}s_n & \text{if } s_n>0 \text{ and } s_n>s_{n+1}\\ 1 & \text{otherwise}\ ,\end{cases} \tag{A5}$$

it is clear that

$$\langle s_n'\rangle=\langle t_n\rangle\ , \tag{A6}$$

which together with

$$\langle s_n'\rangle<\langle 1+s_n\rangle\ , \tag{A7}$$

yields the result

$$\rho^{-1}<\mu\ . \tag{A8}$$

To establish an upper bound on μ, consider the set of steps such that $s_n>0$, which is some fraction g of the interface length in lattice units. Let g' be the fraction such that $s_{n'}=s_n$. Dividing the fraction g into three parts:

$$\begin{aligned}H&=g-g'\ ,\\ L&=g-g'\ ,\\ P&=2g'-g\ ,\end{aligned} \tag{A9}$$

where H is the fraction of steps such that $s_n>s_{n-1}$, L such that $s_n<s_{n+1}$ and P such that $s_n=s_{n+1}$. We now have the expressions

$$\langle t_n\rangle=(1-g')+(2g'-g)\langle s_n\rangle_p+(g-g')\langle s_n\rangle_H\ , \tag{A10}$$

$$\langle s_n\rangle=(2g'-g)\langle s_n\rangle_p+(g-g')\langle s_n\rangle_H+(g-g')\langle s_n\rangle_L\ , \tag{A11}$$

from which we get

$$\mu-1\le 2(g'-1+\rho^{-1})\ , \tag{A12}$$

which with $g'\le 1$ gives

$$\mu\le 2\rho^{-1}+1\ . \tag{A13}$$

[1]M. Eden, *Proceedings of the Fourth Berkeley Symposium on Mathematical Statistics and Probability, Berkeley, California,* edited by F. Neyman (University of California, Berkeley, 1961), Vol. 4, p. 223.
[2]T. A. Witten and L. M. Sander, Phys. Rev. Lett. **47**, 1400 (1982); Phys. Rev. B **27**, 1119 (1983).
[3]P. Meakin, Phys. Rev. Lett. **51**, 1119 (1983).
[4]M. Kolb, R. Botet, and R. Jullien, Phys. Rev. Lett. **51**, 1123 (1983).
[5]M. J. Vold, J. Colloid Interface Sci. **18**, 684 (1963).
[6]D. N. Sutherland, J. Colloid Interface Sci. **22**, 300 (1966).
[7]B. B. Mandelbrot, *The Fractal Geometry of Nature* (Freeman, San Francisco, 1982).
[8]P. Meakin, J. Colloid Interface Sci. **105**, 240 (1985).
[9]D. Bensimon, B. Shraiman, and S. Liang, Phys. Lett. **102A**, 238 (1984).
[10]R. C. Ball and T. A. Witten, Phys. Rev. A **29**, 2966 (1984).
[11]D. N. Sutherland and I. Goodarz-Nia, Chem. Eng. Sci. **26**, 2071 (1971).
[12]L. X. Finegold, Biochim. Biophys. Acta. **448**, 393 (1976); J. H. Donnell and L. X. Finegold, Biophys. J. **35**, 783 (1981).
[13]M. J. Vold, J. Colloid Sci. **14**, 68 (1959); M. J. Vold, J. Phys. Chem. **63**, 1608 (1959).
[14]T. Hashimoto, J. Phys. Soc. Jpn. **41**, 454 (1976).
[15]H. J. Leamy, G. H. Gilmer, and A. G. Dirks, in *Current Topics in Materials Science,* edited by E. Katdis (North-Holland, Amsterdam, 1980), p. 309.
[16]B. A. Orlowski, W. E. Spicer, and A. D. Baer, Thin Solid Films **34**, 31 (1975).
[17]N. G. Nakhodkin, A. I. Shaldervan, A. K. Bardamid, and S. P. Chemakin, Thin Solid Films **34**, 21 (1976).
[18]J. M. Nieuwenheuzen and H. B. Haanstra, Philips Tech. Rev. **27**, 87 (1966).
[19]H. J. Leamy and A. G. Dirks, J. Appl. Phys. **49**, 3430 (1978).
[20]D. Henderson, M. H. Brodsky, and P. Chaudhari, Appl. Phys. Lett. **25**, 641 (1974).
[21]A. G. Dirks and H. J. Leamy, Thin Solid Films **47**, 219 (1977).
[22]H. Konig and G. Helwig, Optik (Stuttgart) **6**, 111 (1950).
[23]R. Ramanlal and L. M. Sander, Phys. Rev. Lett. **54**, 1828 (1985).
[24]T. Hashimoto, K. Okamoto, K. Hara, M. Kamiya, and H. Fujiwara, Thin Solid Films **91**, 145 (1982).
[25]K. H. Guenther, Proceedings of SPIE Meeting, Arlington, Virginia, 1982 (unpublished).
[26]M. Plischke and Z. Racz, Phys. Rev. Lett. **53**, 415 (1984); Phys. Rev. A **32**, 3825 (1985).
[27]F. Family and T. Vicsek, J. Phys. A **18**, L75 (1985).
[28]R. Jullien and R. Botet, Phys. Rev. Lett. **54**, 2055 (1985); J. Phys. A **18**, 2279 (1985).
[29]P. Freche, D. Stauffer, and H. E. Stanley, J. Phys. A **18**, L1163 (1985).
[30]P. Meakin, R. Jullien, and R. Botet, Europhys. Lett. **1**(12), 609 (1986).
[31]R. Hirsch and D. E. Wolf (unpublished).
[32]M. Kardar, G. Parisi, and Y.-C. Zhang, Phys. Rev. Lett. **56**, 889 (1986).
[33]P. Meakin, in *On Growth and Form: Fractal and Nonfractal Patterns in Physics,* edited by H. E. Stanley and N. Ostrowsky (Plenum, New York, 1986).
[34]B. Mandelbrot, in *Fractals in Physics,* edited by L. Pietronero and E. Tossati (Elsevier, Amsterdam, 1986).
[35]S. Alexander, *Proceedings of the Conference on Transport and Relaxation Processes in Random Materials, Gaithersburg, Maryland,* edited by M. Schlsinger and Y. Klafter (World-Scientific, Singapore, 1986).
[36]B. Sutherland, Phys. Lett. **26A**, 532 (1968).
[37]H. V. Beijeren, Phys. Rev. Lett. **38**, 993 (1977).
[38]S. T. Chui and J. D. Weeks, Phys. Rev. B **14**, 4978 (1976).

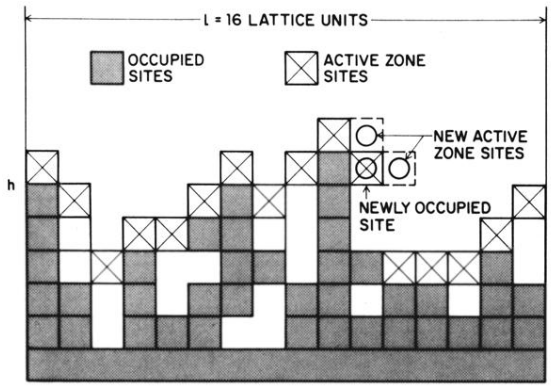

FIG. 1. Schematic representation of a small-scale simulation of ballistic deposition onto a line using a square lattice. Sites occupied by the original surface and the growing deposit are shaded and the sites in the active zones are indicated by crosses. Periodic boundary conditions are used in these simulations and are explicitly shown in the figure. If the site indicated by a cross and a circle is the next to be occupied the two sites indicated by circles alone become new active zone sites and the old active zone sites at the same position (but lower height) disappear from the active zone.

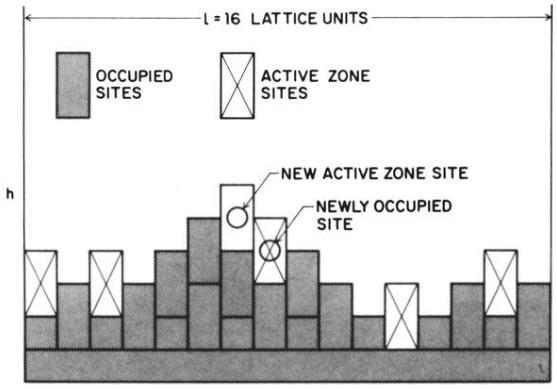

FIG. 2. Schematic representation of a small-scale simulation carried out using the single-step ballistic-deposition model on a square lattice. The sites are labeled in the same way as those in Fig. 1.